2001 December 5

VLBA Scientific Memorandum 28
The AGN Content in the Radio Regime of the NOAO Deep Wide-Field Survey of the Boötes Field: The Pilot VLBA Survey

J. M. Wrobel, G. B. Taylor, and S. T. Myers

National Radio Astronomy Observatory,
P.O. Box O, Socorro, New Mexico 87801, USA

jwrobel@nrao.edu,gtaylor@nrao.edu,smyers@nrao.edu

and

C. D. Fassnacht

Space Telescope Science Institute,
3700 San Martin Drive, Baltimore, MD 21218

cdf@stsci.edu

ABSTRACT

The NRAO VLBA was used at 5.0 GHz to image 27 FIRST sources in the Boötes ($14^{\rm h}$) field of the NOAO Deep Wide-Field Survey (NDWFS). The FIRST sources were selected as being compact and bright enough to have typical position errors in one dimension of ±400 mas at 4σ. For each FIRST source, this *a priori* position error defines the VLBA search region in a phase-referenced image with a FWHM resolution of 3.3 mas by 1.5 mas. FIRST images of these 27 sources imply that 24 are candidates for containing active galactic nuclei (AGN). Five of these AGN candidates were detected with the VLBA above a typical 6σ threshold of 1.5 mJy beam^{-1} and with a position error in one dimension of ±1.5 mas at 1σ. Each VLBA detection has a brightness temperature greater than 10^7 K and must therefore be an AGN. NDWFS images from data release 1.0 suggest that two of these AGN are hosted by galaxies, while two are probable QSOs. NDWFS images are not yet available for the fifth AGN, a possible compact symmetric object. The 19 AGN candidates not detected with the VLBA could still harbor AGN weaker than 1.5 mJy beam^{-1} at 5.0 GHz. Therefore, the AGN content in the radio regime of the Boötes field is at least $21\pm9\%$. Among the 3 FIRST sources that are not AGN candidates, none were detected with the VLBA.

The strategies developed for this pilot VLBA survey of the Boötes field of the NDWFS can be applied to any region of the North Galactic Cap covered by the FIRST

survey, with ancillary photometric and spectroscopic data drawn from the Sloan Digital Sky Survey. Tens of thousands of FIRST sources can therefore be filtered for AGN with the VLBA, opening a new era in the study of radio source populations at milliarcsecond resolution.

Subject headings: astrometry – galaxies: active – quasars: general – radio continuum: galaxies – surveys

1. MOTIVATION

The NOAO Deep Wide-Field Survey (NDWFS) is an imaging survey of 18 square degrees with 5σ detection thresholds in the optical of 26 AB magnitudes and in the near-infrared of 21 AB magnitudes (Jannuzi & Dey 1999). The primary scientific goals of the survey are (1) to study the extent, nature, and evolution of large scale structure at redshifts $z \sim 1 - 4$; (2) to identify rare, luminous star–forming galaxies at $z \gtrsim 4$; and (3) to find the cosmologically important old elliptical galaxies and dusty protogalaxies at $z > 1$. The NDWFS data products will, ultimately, provide photometric and astrometric information on millions of discrete sources. Which of these discrete sources harbor active galactic nuclei (AGN)? A complete census demands a multiwavelength approach, possible because of the careful design of the NDWFS: the survey is split into two fields, each covering 9 square degrees and centered in the constellations of Cetus ($02^{\rm h}$) and Boötes ($14^{\rm h}$), with each field selected as being suitable for complementary observations across the electromagnetic spectrum.

This document reports on an initial AGN inventory of the Boötes field of the NDWFS, based on the flux density and compactness of the radio continuum emission as measured by the brightness temperature $T_{\rm b}$. Specifically, the NRAO Very Long Baseline Array (VLBA) can be used to apply a brightness temperature filter for AGN in the NDWFS, employing the empirical finding that sources with $T_{\rm b} \sim 10^5$ K or higher are too compact to be starbursts and must therefore be driven by AGN (Condon 1992). Each NDWFS field is included in the NRAO Very Large Array survey to produce Faint Images of the Radio Sky at Twenty Centimeters (FIRST) at an angular resolution of about $5''$ and finding about 90 sources per square degree with intensities $S_{\rm peak} > 1$ mJy beam^{-1} at 1.4 GHz (Becker, White, & Helfand 1995; White et al. 1997). For the VLBA survey in the Boötes field, FIRST sources were selected as being compact ($\Theta_M < 5''$) and bright ($S_{\rm peak} > 10$ mJy beam^{-1}). The sky distribution of the resulting 100 sources is shown in Figure 1.

A FIRST source at the 10-mJy level is too weak to be imaged with the VLBA if just traditional self-calibration techniques are applied. However, the prospects for successfully imaging such FIRST sources with the VLBA are good if phase-referencing techniques are employed (Beasley & Conway 1995; Wrobel et al. 2000). Section 2 reports the detection of 5 FIRST sources with the VLBA at 5.0 GHz, using phase-referenced observations of 27 FIRST sources in the North-West quadrant of the Boötes field. The FIRST properties of these 27 are listed in Table 1. Analysis of the FIRST

images implies 24 sources are AGN candidates, 2 sources are hotspots within an extended source, and 1 source is a jet-like feature adjacent to an AGN candidate. Section 3 examines the implications of these VLBA detections.

2. OBSERVATIONS, CALIBRATION, AND IMAGING

The VLBA (Napier et al. 1994) was used to observe the 27 FIRST sources and calibrators on 2001 April 26 UT. Data were acquired in dual circular polarizations with 4-level sampling and at a center frequency 4.98749 GHz with bandwidth 32 MHz. This bandwidth was synthesized from 4 contiguous baseband channels, each of width 8 MHz. Phase-referenced observations were made in the nodding style at elevations above about 10°. Successive 80-second observations of three FIRST sources were preceded and followed by a 60-second observation of the phase, rate, and delay calibrator J1426+3625 (JVAS, Patnaik et al. 1992), leading to a switching time of 5 minutes. Switching angles between this phase calibrator and a FIRST source were 2.0° or less, so only 27 FIRST sources in the North-West quadrant of the NDWFS were reached (Figure 1). Each FIRST source was observed during 6 snapshots spread over time to enhance coverage in the (u, v) plane. Calibrators J1416+3444 (JVAS, Wilkinson et al. 1998) and F14543631 (CLASS, Myers et al. 2001) were observed to check the astrometric accuracy, while calibrators 3C 279 and OQ 208 (Ma et al. 1998) were observed for polarization calibration and to align the phases of the independent baseband channels. Observation and correlation assumed a coordinate equinox of 2000. Positions for the phase calibrator and the astrometric check calibrators were from the first extension (N. R. Vandenberg, 2000, private communication) of the International Celestial Reference Frame (ICRF) as realized by VLBI (Ma et al. 1998). Data editing and calibration were done using the 2001 December 31 release of the NRAO AIPS software and following the strategies outlined by Ulvestad (2001). Data deletion was based on system flags recorded at observation and tape weights recorded at correlation. VLBA system temperatures and gains were used to set the amplitude scale to an accuracy of about 5%, after first correcting for sampler errors.

The AIPS task IMAGR was used to form dirty VLBA images of the Stokes I, Q, and U emission from each FIRST source, with the visibility data being naturally weighted to optimize image sensitivity. Each VLBA image spanned 4096 × 0.4 mas = 1600 mas in each coordinate. Columns 1-4 in Table 1 characterize the parameters of the elliptical Gaussian fit to each FIRST source (White et al. 1997): the peak position coded as the name, the peak intensity ($S_{\rm peak}$), the rms noise value ($\sigma_{\rm s}$), and the major and minor axes dimensions and elongation position angle at FWHM ($\Theta_{\rm M}$, $\Theta_{\rm m}$, PA). These parameters can be used to estimate the 4σ error ellipse for the FIRST position (White et al. 1997). This error ellipse, given in Column 5 of Table 1, defines the VLBA search region. This region is well within the field-of-view (FOV) limits set by time and bandwidth averaging or by non-coplanar baselines (Wrobel 1995). The most constraining FOV limit follows from accepting a 10% drop in the peak amplitude of a true point source due to averaging over each 8-MHz baseband channel; the resulting FOV is elliptical with major axis 3300 mas, minor axis

1500 mas, and elongation PA 0°. Garrington, Garrett, & Polatidis (1999) have developed a similar, but two-stage, strategy for surveying FIRST sources: in the first stage, filtering observations are made with MERLIN at 5 GHz; in the second stage, only the MERLIN detections, with their smaller search ellipses, are targeted during joint observations at 5 GHz with the VLBA plus the European VLBI Network.

For a typical VLBA image, the angular resolution was characterized as an elliptical Gaussian with FWHM dimensions of 3.3 mas by 1.5 mas and elongation PA of 0°. Column 6 of Table 1 gives the rms noise values in the dirty VLBA images at 5.0 GHz of Stokes I ($\sigma_{\rm s}{}^{\rm d}$). These values closely match those expected given the array and observation parameters (Wrobel & Walker 1999). The enormous number of beam areas searched, typically 10^5, requires a $6\sigma_{\rm s}{}^{\rm d}$ threshold for detections (Wall 1979). Residual errors in the phase calibration will degrade the point-source sensitivity of the VLBA. To quantify the effect of this loss of coherence, after phase self-calibration the images of the calibrators J1416+3444 and F14543631 had peak intensities of 1.21 and 1.07, respectively, times their peak intensities before phase self-calibration. Observations of these calibrators required switching angles of $1-3°$. But switching angles of $1-2°$ were needed to reach the FIRST sources, so the appropriate correction for coherence loss is about 1.15 and the upper limits ($S_{\rm peak}^{\rm d}$) in Column 7 of Table 1 are set to $1.15 \times 6\sigma_{\rm s}{}^{\rm d}$.

Five dirty images of Stokes I at 5.0 GHz showed peaks above the detection threshold of $6\sigma_{\rm s}{}^{\rm d}$. These images were cleaned using the AIPS task IMAGR in regions centered on the detections and spanning 8 mas for the isolated detections and 16 mas for the double detection. Figure 2 shows these cleaned images, while Table 2 lists results from analyzing the 6 components in the images at 5.0 GHz. Column 3 gives the rms noise values ($\sigma_{\rm s}{}^{\rm c}$). Quadratic fits to the components yielded the peak intensities ($S_{\rm peak}^{\rm c}$) in Column 4 plus the peak positions in Column 5 ($\alpha_{\rm J2000}$) and Column 6 ($\delta_{\rm J2000}$). The errors in the peak intensities are the quadratic sums of the image rms values and a 5% scale error. Column 7 gives the astrometric error in one dimension ($\sigma_{\rm a}{}^{\rm c}$), taken to be the quadratic sum of terms measuring the peak signal-to-noise ratio (Ball 1975) and the accuracy of the absolute astrometry. Images of the calibrators J1416+3444 and F14543631 prior to phase self-calibration set the latter term to 1.5 mas, large enough to dominate the position error budget. The components in Figure 2 seem to be slightly resolved, but this apparent resolution is likely to be artifical and due to residual errors in the phase calibration. Conservative upper limits to the major and minor diameters of each component are 3.3 mas and 1.5 mas, respectively. For the stronger sources, areal integrations were done over N beam areas to estimate the total flux densities ($S_{\rm total}^{\rm c}$) listed in Column 8, for which the associated errors are the quadratic sums of $\sqrt{N}$ times the image rms values and a 5% scale error. Each of the 6 components in Table 2 has a linearly polarized flux density below 1 mJy beam^{-1}. This limit is of physical interest only for J142910.223+352946.86, for which the corresponding polarization percentage is less than 7%.

VLBA phase-referenced data were also acquired on 2000 September 8 UT at a center frequency of 8.42149 GHz, but otherwise employing identical observing strategies. The utility of those data for search purposes was compromised by the elevated system temperatures due to rain at 4 anten-

nas; the substantial coherence loss correction of about 1.4; and the larger number of synthesized beam areas, with major and minor axes at FWHM of 2.0 mas and 0.9 mas, respectively, in the search ellipses. Still, for the 5 VLBA detections at 5.0 GHz, the dirty images at 8.4 GHz resulted in detections of J142456.287+352841.80 and J142910.223+352946.86, plus upper limits for J142842.556+354326.60 (< 2.6 mJy beam^{-1}), J142937.566+344115.69 (< 2.8 mJy beam^{-1}), and J143449.111+354246.98 (< 3.2 mJy beam^{-1}). Analysis of cleaned images of the two detections yielded the entries at 8.4 GHz in Table 2.

3. IMPLICATIONS

Twenty-four FIRST sources are AGN candidates. Five of these were detected with the VLBA at 5.0 GHz above a typical threshold of 1.5 mJy beam^{-1}. Four of the VLBA detections are isolated components (J142456.287+352841.80, J142842.556+354326.60, J142910.223+352946.86, and J142937.566+344115.69), while the fifth VLBA detection is a double (J143449.111+354246.98). Each detected component has major and minor diameters less than 3.3 mas and 1.5 mas, respectively. The corresponding brightness temperatures are $T_{\rm b} > 10^7$ K. Free-free absorption limits the total brightness temperature of the coextensive thermal and nonthermal radio sources generated by any starburst to a few times the electron temperature of about 10^4 K at frequencies above about 1 GHz (Condon 1992). The VLBA detections with $T_{\rm b} > 10^7$ K are too compact to be starbursts and must, therefore, be driven by AGN. While an unusually powerful radio supernova in a nearby galactic nucleus could mimic an AGN for a few months or years (eg, Wrobel, Fassnacht, & Ho 2001), such a supernova would remain undetected at the cosmological distances suggested below for these 5 FIRST sources. The VLBA astrometry of these 5 AGN anchors the Boötes field of the NDWFS to the ICRF.

NDWFS images in B_w, R, and I are available from data release 1.0 for 4 of the 5 VLBA detections. Profile fitting was done to these images to assess the optical counterparts' spatial extents, total magnitudes in I (Column 2, Table 3), and typical colors $B_w - R$ and $R - I$ (Column 3-4, Table 3). J142456.287+352841.80 and J142910.223+352946.86 are each probably a QSO, being both blue and spatially unresolved in the NDWFS. J142456.287+352841.80 is fainter, and probably more distant, than the FIRST quasars identified by Becker et al. (2001). J142842.556+354326.60 and J142937.566+344115.69 are each probably a galaxy, being spatially resolved in the NDWFS. J142842.556+354326.60 is redder in $R - I$ than any of the galaxy tracks through the color-color diagram in Jannuzi & Dey (1999). The galaxy type is most likely elliptical, in which case it may be at a photometric redshift $z_{\rm ph} \sim 1 - 2$. J142937.566+344115.69, although weak, has colors that are consistent with several galaxy tracks: it could be a Sc galaxy at $z_{\rm ph} \sim 1$, a Sb galaxy at $z_{\rm ph} \sim 1.5$, or an elliptical galaxy at $z_{\rm ph} \sim 2.5$. But these estimated photometric redshifts must be quite unreliable: they are based on no-evolution models and are therefore inapplicable for redshifts beyond 0.5 or so. NDWFS images are not yet available for the fifth VLBA dectection, J143449.111+354246.98, suspected of being a compact symmetric object. Ancillary optical data

will be particularly valuable in this case, because these young (Owsianik, Conway, & Polatidis 1998; Taylor et al. 2000) and rare objects offer insights into evolutionary models for radio galaxies (Readhead et al. 1996) and strong tests of unified schemes for AGN (Peck et al. 2000).

The 19 AGN candidates not detected with the VLBA could still harbor AGN weaker than 1.5 mJy beam^{-1} at 5.0 GHz. Therefore, the AGN content in the radio regime of the Boötes field is at least 21±9%. The statistical accuracy of this result is set by the small numbers of AGN candidates observed and detected in this pilot VLBA survey. When complete, the VLBA survey will target about four times as many AGN candidates. This will improve measures of the AGN content and enable meaningful comparisons with the predictions of evolutionary models for radio source populations, such as the promising one by Jackson & Wall (1999) based on a unification scheme. More VLBA detections will also help broaden knowledge of the range of structures in samples unbiased by spectral preselection. This could potentially lead to the discovery of new types of VLBA sources and also have implications for the interpretation of VLBA images of sources thought to be gravitationally lensed (eg, Augusto et al. 2001). Further VLBA nondections of AGN candidates will still have astrophysical value, because of the visibility-function constraints on mas scales and the ancillary identification information. Analysis of these topics for all undetected AGN candidates will be deferred until the VLBA survey of the Boötes field is complete.

Among the 3 FIRST sources in the pilot survey that are not AGN candidates, none were detected with the VLBA. This is as expected, as 2 of these are hotspots in a Fanaroff-Riley class II source, while the third is a jet-like feature adjacent to an undetected AGN.

The strategies developed for this pilot VLBA survey of the Boötes field of the NDWFS can be applied to any region of the North Galactic Cap covered by the FIRST survey, with ancillary photometric and spectroscopic data drawn from the Sloan Digital Sky Survey (York et al. 2000). Tens of thousands of FIRST sources can therefore be filtered for AGN with the VLBA, opening a new era in the study of radio source populations at milliarcsecond resolution.

Positions of calibrators in the first extention of the ICRF were provided by observations from the joint NASA/USNO/NRAO geodetic/astrometric observing program. This work made use of images provided by the NOAO Deep Wide-Field Survey (Jannuzi & Dey 1999), which is supported by NOAO. NOAO is operated by AURA, Inc., under a cooperative agreement with the National Science Foundation. NRAO is a facility of the National Science Foundation operated under cooperative agreement by Associated Universities, Inc.

REFERENCES

Augusto, P., et al. 2001, MNRAS, 326, 1007

Ball, J. A. 1975, in Methods in Computational Physics, Volume 14, eds. B. Alder, S. Fernbach, & M. Rotenberg (New York: Academic Press), 177

Beasley, A. J., & Conway, J. E. 1995, in ASP Conf. Ser. 82, Very Long Baseline Interferometry and the VLBA, eds. J. A. Zensus, P. J. Diamond, & P. J. Napier (San Francisco: ASP), 327

Becker, R. H., White, R. L., & Helfand, D. J. 1995, ApJ, 450, 559

Becker, R. H., et al. 2001, ApJS, 135, 227

Condon, J. J. 1992, ARA&A, 30, 575

Garrington, S. T., Garrett, M. A., & Polatidis, A. 1999, New Astronomy Reviews, 43, 629

Jackson, C. A., & Wall, J. V. 1999, MNRAS, 304, 160

Jannuzi, B. T., & Dey, A. 1999, in Photometric Redshifts and High Redshift Galaxies, ed. R. J. Weymann et al. (San Francisco: ASP), 111

Ma, C., et al. 1998, AJ, 116, 516

Myers, S. T., et al. 2001, in preparation

Napier, P. J., Bagri, D. S., Clark, B. G., Rogers, A. E. E., Romney, J. D., Thompson, A. R., & Walker, R. C. 1994, Proc. IEEE, 82, 658

Owsianik, I., Conway, J. E., & Polatidis, A. G. 1998, A&A, 336, L37

Patnaik, A. R., Browne, I. W. A., Wilkinson, P. N., & Wrobel, J. M. 1992, MNRAS, 254, 655

Peck, A. B., Taylor, G. B., Fassnacht, C. D., Readhead, A. C. S., & Vermeulen, R. C. 2000, ApJ, 534, 104

Readhead, A. C. S., Taylor, G. B., Pearson, T. J., & Wilkinson, P. N., 1996, ApJ, 460, 634

Taylor, G. B., Marr, J. M., Readhead, A. C. S., & Pearson, T. J. 2000, ApJ, 541, 112

Ulvestad, J. S. 2001, VLBA Scientific Memorandum 25

Wall, J. V. 1979, QJRAS, 20, 18

White, R. L., Becker, R. H., Helfand, D. J., & Gregg, M. D. 1997, ApJ, 475, 479

Wilkinson, P. N., Browne, I. W. A., Patnaik, A. R., Wrobel, J. M., & Sorathia, B. 1998, MNRAS, 300, 790

Wrobel, J. M. 1995, in ASP Conf. Ser. 82, Very Long Baseline Interferometry and the VLBA, eds. J. A. Zensus, P. J. Diamond, & P. J. Napier (San Francisco: ASP), 413

Wrobel, J. M., & Walker, R. C. 1999, in ASP Conf. Ser. 180, Synthesis Imaging in Radio Astronomy II, eds. G. B. Taylor, C. L. Carilli, & R. A. Perley (San Francisco: ASP), 171

Wrobel, J. M., Walker, R. C., Benson, J. M, & Beasley, A. J., 2000, VLBA Scientific Memorandum 24

Wrobel, J. M., Fassnacht, C. D., & Ho, L. C. 2001, ApJ, 553, L23

York, D. G., et al. 2000, AJ, 120, 1579

Table 1. Photometry and Astrometry of FIRST Sources

	VLA at 1.4 GHz				VLBA at 5.0 GHz	
FIRST Name	$S_{\rm peak}$ (mJy beam^{-1})	$\sigma_{\rm s}$ (mJy beam^{-1})	$\Theta_{\rm M}$,$\Theta_{\rm m}$,PA ($''$,$''$,$^\circ$)	Search Ellipse (mas,mas,$^\circ$)	$\sigma_{\rm s}{}^{\rm d}$ (mJy beam^{-1})	$S_{\rm peak}{}^{\rm d}$ (mJy beam^{-1})
(1)	(2)	(3)	(4)	(5)	(6)	(7)
AGN Candidates						
J142456.287+352841.80	11.32	0.141	1.36,0.00,118.4	852,826,118.4	0.25	3.0
J142516.512+345246.62	57.30	0.136	2.50,0.27,147.6	760,691,147.6	0.24	<1.7
J142632.164+350814.71	87.10	0.134	2.09,1.10, 70.3	728,693, 70.3	0.25	<1.7
J142705.073+343628.84	27.03	0.133	2.34,0.48,176.5	789,727,176.5	0.26	<1.8
J142738.271+343148.69	46.80	0.141	3.39,2.23,121.4	825,756,121.4	0.24	<1.7
J142842.556+354326.60	19.16	0.142	1.57,1.25, 65.9	789,777, 65.9	0.25	2.3
J142904.545+343243.54	12.23	0.145	1.72,0.54,178.6	858,822,178.6	0.24	<1.7
J142905.666+3449 9.87	25.83	0.137	3.65,0.70,168.6	880,735,168.6	0.23	<1.6
J142906.607+354234.67	29.73	0.143	0.69,0.00,148.5	728,722,148.5	0.26	<1.8
J142910.223+352946.86	17.49	0.140	0.75,0.70, 90.0	773,772, 90.0	0.59	14.6
J142937.566+344115.69	10.60	0.135	1.34,0.49,179.7	856,834,179.7	0.25	1.6
J143008.885+344713.75	26.74	0.145	0.88,0.80, 0.0	740,739, 0.0	0.23	<1.6
J143022.337+343727.14	11.28	0.132	1.85,1.03,111.6	863,831,111.6	0.23	<1.6
J143134.549+351511.19	58.47	0.137	1.91,1.42,133.2	731,713,133.2	0.24	<1.7
J143155.856+345926.99	10.53	0.142	1.32,0.27, 66.0	865,842, 66.0	0.24	<1.7
J143213.543+350941.05	15.65	0.146	1.57,0.00, 23.1	816,783, 23.1	0.25	<1.7
J143237.978+353036.69	13.89	0.139	4.17,1.01,145.4	1002,807,145.4	0.24	<1.7
J143239.561+350151.42	12.86	0.145	1.12,0.84, 0.0	827,820, 0.0	0.24	<1.7
J143256.072+353339.52	62.94	0.131	0.65,0.14, 90.0	691,686, 90.0	0.25	<1.7
J143259.904+352833.52	13.47	0.140	3.77,1.29,175.6	973,820,175.6	0.24	<1.7
J143309.671+351520.14	13.77	0.146	2.66,0.90,141.0	893,812,141.0	0.24	<1.7
J143432.836+352141.47	20.32	0.130	1.96,1.64, 24.5	791,777, 24.5	0.24	<1.7
J143435.361+352622.26	30.93	0.132	0.82,0.55, 0.0	723,719, 0.0	0.26	<1.8
J143449.111+354246.98	21.57	0.143	1.38,0.00,128.4	771,747,128.4	0.33	4.3
Other						
J142617.948+344039.63	11.88	0.141	2.22,1.68, 64.1	885,857, 64.1	0.25	<1.7
J142623.374+343950.45	16.61	0.138	1.38,0.00, 68.6	794,770, 68.6	0.25	<1.7
J143433.725+352128.50	10.97	0.130	4.92,1.71,141.9	1107,858,141.9	0.25	<1.7

Table 2. VLBA Components at 5.0 and 8.4 GHz

FIRST Name (1)	Frequency (GHz) (2)	σ_s[c] (mJy beam^{-1}) (3)	S_{peak}[c] (mJy beam^{-1}) (4)	α_{J2000} (h,m,s) (5)	δ_{J2000} (°,′,″) (6)	σ_a[c] (mas) (7)	S_{total}[c] (mJy) (8)
J142456.287+352841.80	5.0	0.23	3.2±0.3	14 24 56.30460	+35 28 41.7473	1.5	3.2±0.8
	8.4	0.31	2.6±0.3	14 24 56.30459	+35 28 41.7474	1.5	—
J142842.556+354326.60	5.0	0.24	2.2±0.3	14 28 42.55564	+35 43 26.9421	1.5	3.6±0.9
J142910.223+352946.86	5.0	0.31	14.8±0.8	14 29 10.22242	+35 29 46.8911	1.5	23.9±1.6
	8.4	0.56	9.5±0.7	14 29 10.22243	+35 29 46.8911	1.5	14.7±2.5
J142937.566+344115.69	5.0	0.24	1.7±0.3	14 29 37.55494	+34 41 15.5915	1.5	—
J143449.111+354246.98	5.0	0.25	4.1±0.3	14 34 49.10159	+35 42 47.2206	1.5	13.5±1.8[a]
	5.0	0.25	3.5±0.3	14 34 49.10185	+35 42 47.2186	1.5	—

[a]Includes both components.

Table 3. Data from NDWFS Release 1.0

FIRST Name (1)	Total I (AB mag) (2)	Typical $B_w - R$ (AB mag) (3)	Typical $R - I$ (AB mag) (4)
J142456.287+352841.80	19.8	−0.9	+0.6
J142842.556+354326.60	19.9	+0.5	+2.5
J142910.223+352946.86	18.4	−1.6	+1.7
J142937.566+344115.69	21.5	+0.1	+1.1

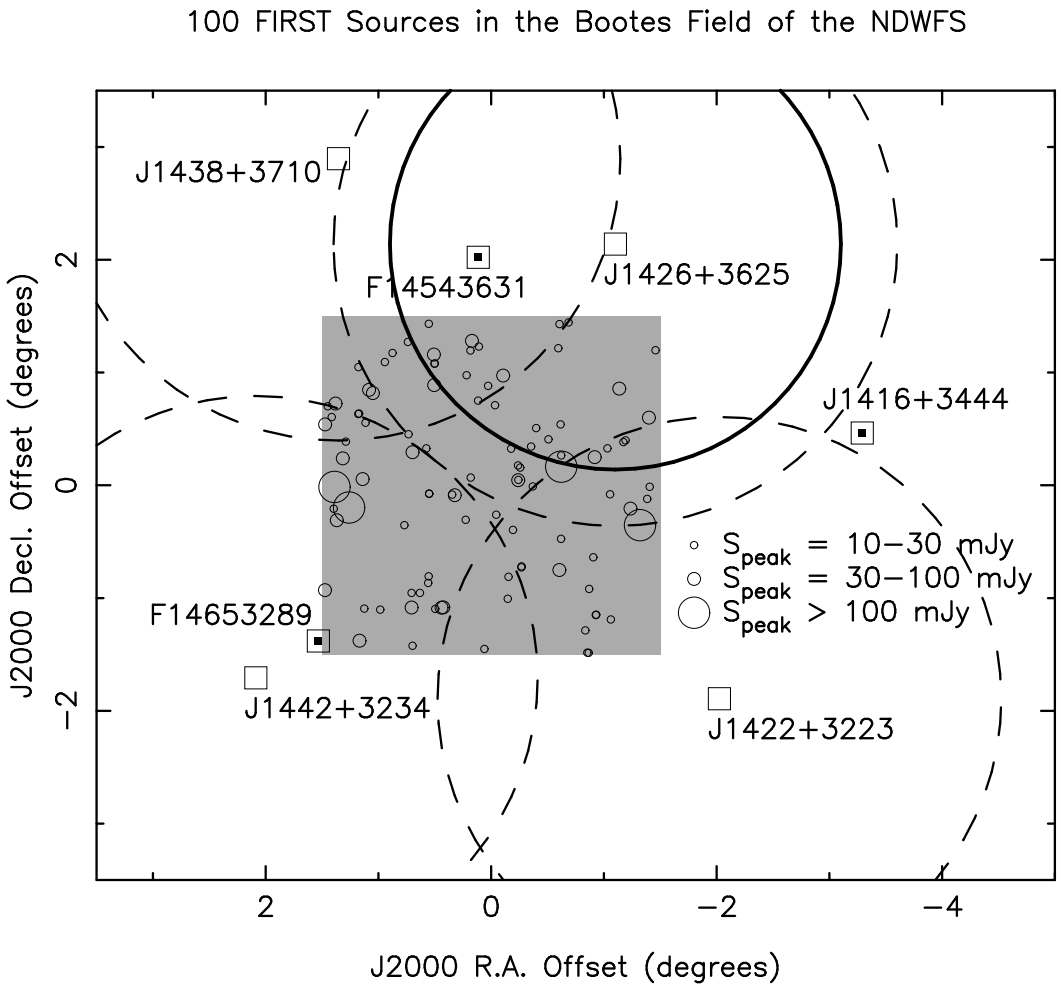

Fig. 1.— Shaded square is 3° on a side and shows the Boötes (14^h) field of the NOAO Deep Wide-Field Survey (NDWFS). The circles in the field show 100 FIRST sources, with bigger circles encoding stronger sources. The calibrators outside the field are marked as simple squares for phase calibrators and as squares with inner symbols for astrometric check sources. The 2 check sources closest to the survey region are weak CLASS sources. A dashed circle of radius 2.5° is centered on each phase calibrator, showing a plausable switching angle for phase referencing at a frequency of 5.0 GHz. Each FIRST source in the Boötes field is therefore accessible to the VLBA. This work reports VLBA results for the 27 FIRST sources located 2.0° or less from the phase calibrator J1426+3625. The thick circle centered on this phase calibrator has a radius of 2.0°.

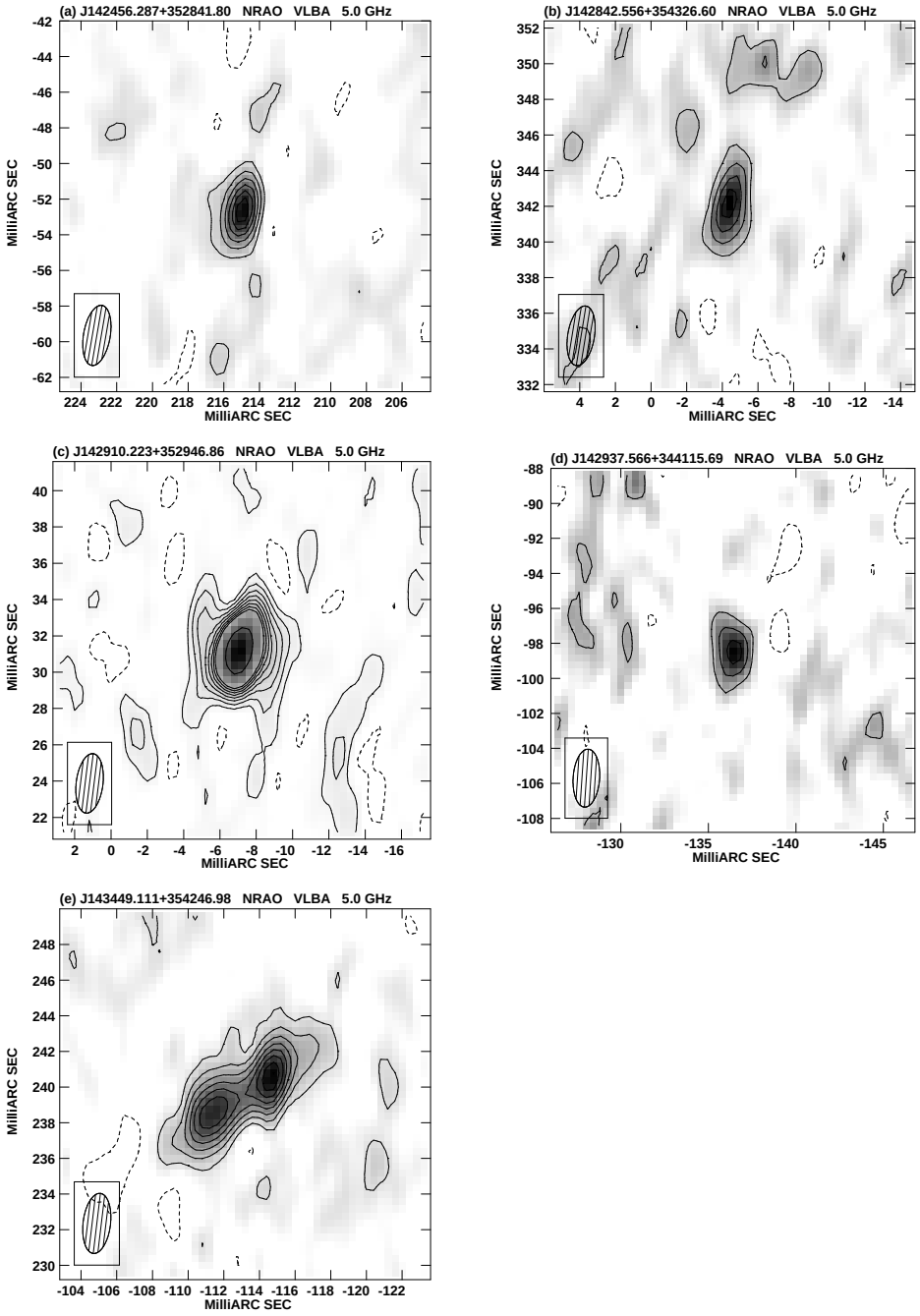

Fig. 2.— Montage of VLBA images of Stokes I emission from 5 FIRST sources detected at a frequency of 5.0 GHz. Each cleaned image is centered on the position of the VLBA detection and spans 20 mas. In each image, the shaded ellipse shows the Gaussian restoring beam at FWHM, negative contours are dashed while positive ones are solid, the grey scale shows positive intensities with darkest values at the image peak (Column 4, Table 2), and contour levels are at -6, -4, -2, 2, 4, 6, 8, 10, 12, 14, and 16 times the rms noise level (Column 3, Table 2). (a) J142456.287+352841.80. (b) J142842.556+354326.60. (c) J142910.223+352946.86. Extra contour level at 32. (d) J142937.566+344115.69. (e) J143449.111+354246.98.